



Enhanced Axial Erosion of the Sputter Cathode in SNICS

J.H. Billen

April 1981

UWFDM-413

FUSION TECHNOLOGY INSTITUTE
UNIVERSITY OF WISCONSIN
MADISON WISCONSIN

DISCLAIMER

This report was prepared as an account of work sponsored by an agency of the United States Government. Neither the United States Government, nor any agency thereof, nor any of their employees, makes any warranty, express or implied, or assumes any legal liability or responsibility for the accuracy, completeness, or usefulness of any information, apparatus, product, or process disclosed, or represents that its use would not infringe privately owned rights. Reference herein to any specific commercial product, process, or service by trade name, trademark, manufacturer, or otherwise, does not necessarily constitute or imply its endorsement, recommendation, or favoring by the United States Government or any agency thereof. The views and opinions of authors expressed herein do not necessarily state or reflect those of the United States Government or any agency thereof.

Enhanced Axial Erosion of the Sputter Cathode in SNICS

J.H. Billen

Fusion Technology Institute
University of Wisconsin
1500 Engineering Drive
Madison, WI 53706

<http://fti.neep.wisc.edu>

April 1981

UWFDM-413

ENHANCED AXIAL EROSION OF THE SPUTTER CATHODE IN SNICS

James H. Billen

Dept. of Physics and Dept. of Nuclear Engineering
University of Wisconsin, Madison, Wisconsin 53706

Summary

Calculations of the electric potential and of Cs^+ -ion trajectories explain the axially enhanced erosion of the sputter cathode in the Wisconsin Source of Negative Ions by Cesium Sputtering (SNICS) and similar sources. The effect arises from purely electrostatic focussing of fast Cs^+ ions that are produced on a hot refractory-metal surface. Calculations which include the effects of a 1-mA Cs^+ beam suggest that space charge is of only minor importance in this type of ion source. Possible improvements in the efficiency of the ionizer that arise from modifications to the source geometry are also discussed.

Introduction

A few years ago a new and very successful sputter-type negative-ion source was developed at Wisconsin^{1,2} and independently at Pennsylvania.³ With appropriate cathode materials these sources produce intense, low-emittance negative-ion beams of elements throughout the periodic table. In SNICS, -2-keV Cs^+ ions sputter the cathode's cesium-coated solid surface. Sputtered negative ions of the cathode material accelerate across the 2-kV cathode-to-anode potential difference and emerge from the exit aperture. The Cs^+ beam of 1-5 mA originates by surface ionization on a hot tungsten helix that is coaxial with the sputter cathode and exit aperture. Different versions of the Pennsylvania source have employed ionizers of a cylindrical, helical and annular shape. A common characteristic of all of these sources is an axially enhanced erosion pattern on the sputter cathode which suggests that the incident Cs^+ beam is tightly focussed. Figure 1 shows several views of an initially flat-faced aluminum cathode after a few days of running.

An earlier attempt² to explain the axial erosion involved the focussing of plasma ions by the electric field and by the magnetic field produced by a direct current in the helical ionizer. Middleton observed, however, the axial erosion even with ionizer geometries that produce no magnetic field. A treatment of the ion source as a surface ionization gauge leads to an estimate for the Cs vapor pressure between 10^{-4} and 10^{-5} Torr, and hence Cs^+ -ion mean free paths that are 5 to 50 times larger than the (~30 mm) dimensions of the source. These considerations suggest that the trajectories of the Cs^+ ions incident on the sputter cathode come directly from the hot W ionizer rather than from a plasma. Results of the calculations presented below support this hypothesis.

Procedure

The calculations that I performed involved several steps. The first step for a particular source geometry was to obtain the electric potential in which the Cs^+ ions move. I assumed cylindrical symmetry and as a first approximation ignored the effects of space charge and magnetic fields. The weak magnetic field produced by the ionizer current in SNICS has a negligible effect

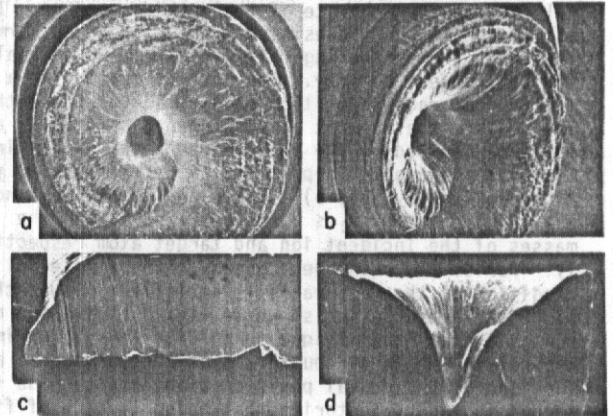


Figure 1. Scanning electron micrographs of an aluminum sputter cathode after several days of running. This cathode was initially a rod 12.7 mm long by 9.5 mm in diameter. Part (a) shows a face-on view and (b) shows the cathode tilted 45°. The cathode was cut through the symmetry axis to show in cross section the erosion along the side (c) and on the face (d). The sputtered hole is about 5 mm deep.

on the massive Cs^+ ions, but it may serve to trap electrons and thereby neutralize some Cs^+ space charge. Figure 2 shows the electric potential that results from

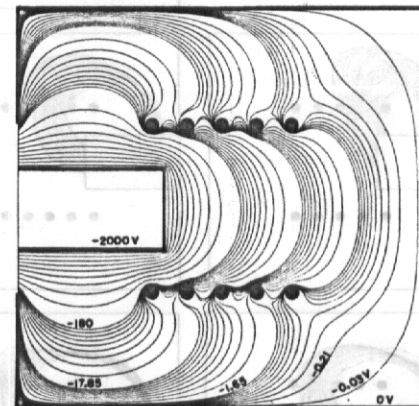


Figure 2. Equipotentials for the SNICS geometry. The chamber dimensions are 30 mm long by 30 mm diameter. Four groups of equipotentials are shown. In the first group nearest the -2000-V sputter cathode the curves differ by 180 volts. In the other three groups the curves differ by 18 V, 1.8 V, and 0.18 V respectively. The 5-turn ionizer and walls are at 0 V. Potentials for a few of the curves are indicated on the figure.

a solution of Laplace's equation in cylindrical coordinates subject to Dirichlet boundary conditions. Five circular hoops at ground potential approximate the 5-turn helix of 1-mm diameter W used in SNICS. I determined the potential on 10^5 mesh points in one of the half planes by the method of successive overrelaxation. The distance between mesh points was 0.067 mm. Next I used a sixth-order Runge-Kutta formula to solve the differential equations of motion and trace the trajectories of Cs^+ ions originating on the ionizer. Figure 3 shows 500 trajectories with origins evenly distributed over the ionizer surface.

The last step in the analysis was to estimate the relative sputtering rate of the cathode surface. If all of the Cs^+ particles struck the cathode at normal incidence the sputtering rate would be proportional to the Cs^+ current density. The current density as a function of radial position on the face of the cathode is equal to the current falling upon a particular annular zone divided by the area of the zone. According to Sigmund⁵ the angular dependence of the sputtering yield is approximately $(\cos \theta)^{-5/3}$ for angles of incidence $\theta \leq 70^\circ$ and for $m_2/m_1 \leq 3$ where m_1 and m_2 are the masses of the incident ion and target atom respectively. For Cs^+ ions incident on any cathode material this condition on the mass ratio is satisfied. Fewer than 1% of the trajectories shown in Fig. 3 strike the cathode at angles more oblique than 70° . Thus to estimate the relative rate of sputtering of the surface as a function of the radial position along the cathode face I counted the trajectories that ended in each of fifteen annular zones with each trajectory weighted by the factor $(\cos \theta)^{-5/3}$ and then divided by the area of the zone.

Cs^+ Trajectories
50% end on face
47% end on side

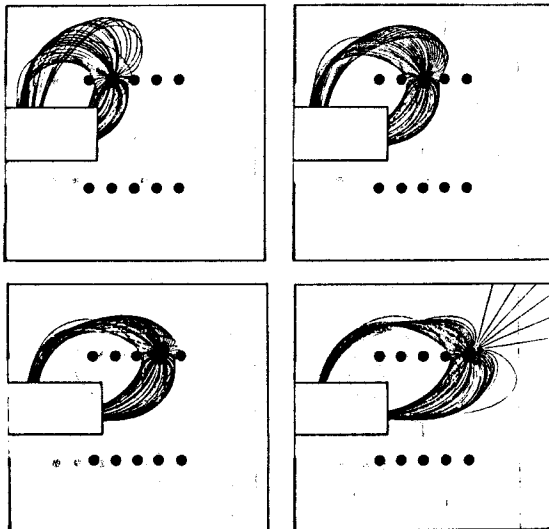
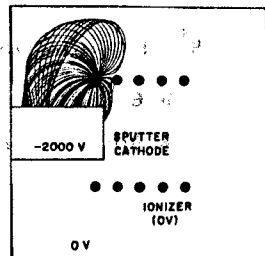


Figure 3. Cs^+ -ion trajectories originating on the 5-turn ionizer of 1-mm tungsten. Each of the five views shows 100 trajectories.

Results

Figure 4 shows the relative sputtering rate that resulted from an analysis of the trajectories shown in Fig. 3. The sputtering rate is very strongly peaked on axis and thus explains the most obvious feature on a worn sputter cathode. An enhancement of the sputtering rate between 1 mm and 2 mm should result in the erosion of a groove in the face of the cathode in addition to the deep central pit. All of our worn cathodes exhibit such a structure but with a spiral shape that probably reflects the helical shape of the ionizer (see Fig. 1). Figure 1(c) shows a groove in the side of the sputter cathode about 8 mm from the face end. This type of erosion is also common to all worn cathodes and is essentially independent of the cathode diameter. An inspection of the trajectories in Fig. 3 indicates that such an erosion pattern is to be expected.

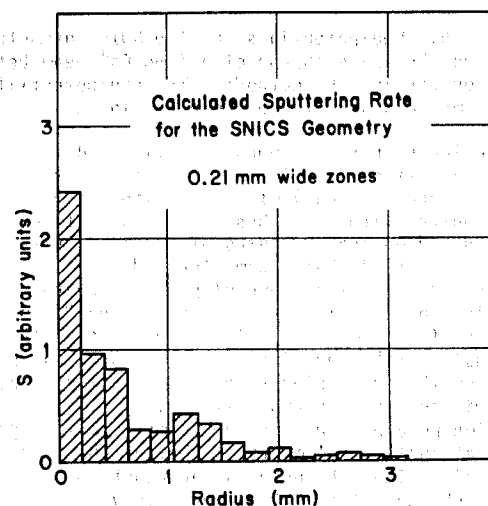


Figure 4. Sputtering rate of the cathode face as a function of radial position. About 18% of the total Cs^+ current falls within the first 3/4 radial zones and hence contributes to the formation of the negative-ion beam.

Effects of Space Charge

The foregoing analysis has neglected the effects of the Cs^+ current's own space charge on the particle trajectories. To assess the possible consequences of ignoring the Cs^+ space charge I solved the Poisson equation:

$$\nabla^2 U(r,z) = -\rho(r,z)/\epsilon_0$$

where $U(r,z)$ is the electric potential and $\rho(r,z)$ is the charge density derived from a set of representative Cs^+ trajectories. A self-consistent potential and set of trajectories resulted after three relaxation calculations of the potential. Each such calculation used the space charge term from the previous iteration's trajectories. I made no attempt to include the space charge from electrons. The presence of electron space charge will tend to neutralize the positive space charge of the Cs^+ ions. Any differences observed between the trajectories with and without Cs^+ space charge may, therefore, be exaggerated.

Figure 5 shows the electric potential that resulted from including the space charge of a 1-mA Cs^+ beam incident on the sputter cathode. The boundary conditions and the equipotentials displayed are the same as those in Fig. 2. Only the equipotentials between -8 V and 0 V (where the slow moving Cs^+ ions contribute an

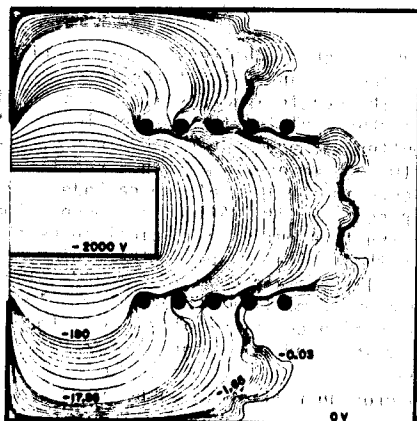


Figure 5. Equipotentials for the SNICS geometry including the space charge of a 1-mA Cs^+ beam between the ionizer and the cathode. The equipotentials are the same values as those shown in Fig. 2.

appreciable charge) showed significant differences from the charge-free potential. About 13% (compared to 3% without space charge) of the Cs^+ ions never reached the sputter cathode. These Cs^+ ions that were "lost" originated on the two turns of the ionizer farthest from the cathode but became trapped near the ionizer by the buildup of a cloud of positive charge. Of the Cs^+ ions originating from the remaining 87% of the ionizer surface about half strike the face of the cathode and half strike the side. Figure 6 shows a comparison between the sputtering rates on the cathode face with and without space charge effects. The axially peaked erosion remained and the enhancement of the sputtering rate at just over 1-mm radius moved toward the symmetry axis. Thus the original approach that neglects space charge effects is adequate in view of the relatively slight modifications that arise from the inclusion of space charge and the likelihood of space charge neutralization by electrons. (Inclusion of the effects of space charge also requires a much larger computational effort.)

Other Geometries

Because of the model's initial success in explaining the gross features of sputter cathode erosion I hoped to use the calculations to improve source performance. One measure of source performance is the efficiency of the ionizer in delivering Cs^+ ions to the region of the sputter cathode from which the negative-ion beam emerges. This region is indeed small. From a calculation of negative-ion trajectories emerging from the cathode face I found that only those trajectories originating within 0.47 mm of the cathode center illuminated a 2-mm diameter exit aperture and hence contributed to the negative-ion beam current. However, once an appreciable conical hole had formed on the cathode, a weak focussing of the negative ions occurred and the beam's source area expanded to a radius of 0.74 mm. The formation of a conical hole has two important and fortuitous effects. First, of course, is the fact that a much larger surface area becomes available for the production of the negative-ion beam. Secondly, since a hole in the cathode face has almost no effect on the incident Cs^+ -ion trajectories, the Cs^+ ions strike the already-eroded surface at more oblique angles than they strike the (initially) flat surface. This further enhances the sputtering rate because of the $(\cos \theta)^{-5/3}$ dependence.

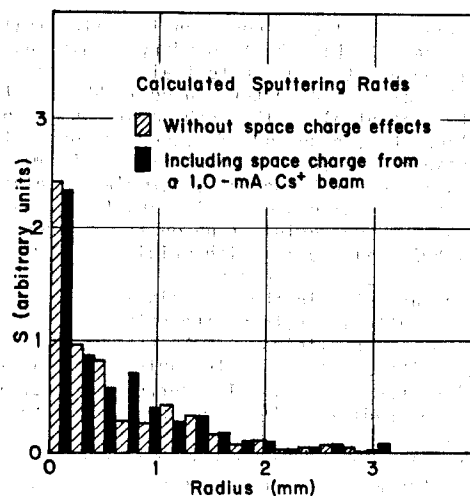


Figure 6. Comparison of the sputtering rate on the cathode face with and without space charge effects. The zone width was 0.21 mm for each calculation.

One improvement in the ionizer efficiency might involve delivering more Cs^+ ions to the first 3 or 4 radial zones of the cathode face (see Fig. 4) for the same ionizer surface area. Figure 7 shows the Cs^+ trajectories that resulted when a mask (at ground potential) was inserted just behind the ionizer to prevent Cs^+ ions from reaching the side of the cathode. Even though 10% of all the Cs^+ particles were lost to the

Cs^+ Trajectories
68% end on face
22% end on side

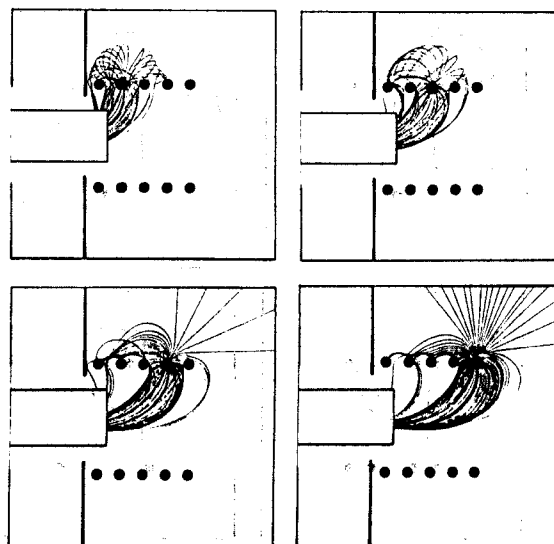
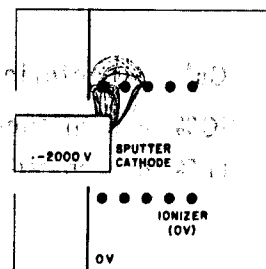


Figure 7. Cs^+ -ion trajectories for the SNICS geometry with the addition of a mask near the ionizer.

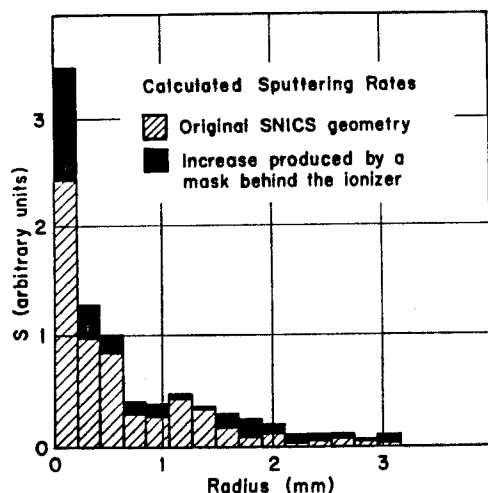


Figure 8. Sputtering rate resulting from the trajectories shown in Fig. 7. With the addition of the mask the ionizer efficiency rose from 18% to 23%.

chamber walls more particles than without the mask reached the cathode face and resulted in the marked increase in the sputtering rate on axis shown in Fig. 8. In spite of this improvement, however, only about 23% of the total Cs^+ beam falls within the first three and one-half zones and contributes to the formation of the negative-ion beam. The corresponding efficiency for trajectories of Fig. 3 (without the mask) is 18%.

An even more favorable geometry is illustrated in Fig. 9. This is a model of Middleton's original ion source³ in which the ionizer was an annulus of rhenium located behind the cathode face. In this example the annular ionizer has about the same total surface area as the five-turn helix used in SNICS. Even though half of the Cs^+ ions cannot strike the cathode face, the overall efficiency of this ionizer approaches 50% because all of the Cs^+ ions from the front face of the annulus fall within 1 mm of the cathode center.

Conclusion

A very simple model involving only electrostatic focussing of fast Cs^+ ions accounts for the behavior of SNICS and similar surface-ionization sputter-type ion sources. With a relatively modest investment of computer time one may investigate and perhaps refine new ideas and modifications before one commits shop time and effort to a project. Further work along these lines continues, particularly to see whether reliable quantitative predictions of the negative-ion beam current and emittance are possible.

Acknowledgements

I wish to thank Prof. H.T. Richards, S. Riedhauser and G.T. Caskey for many helpful discussions and D.B. Bullen for preparing the electron micrographs. I am also grateful to D. Wiltzius and National Electrostatics Corporation for the particle trajectory computer code, PTRAC. This work was supported in part by the U.S. Department of Energy.

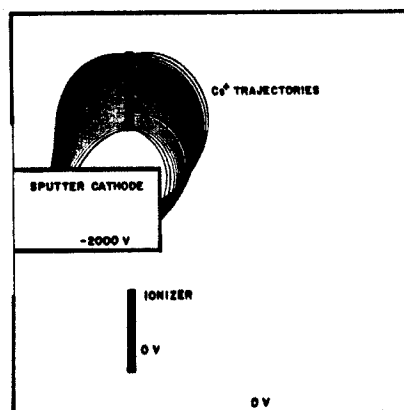


Figure 9. Cs^+ -ion trajectories from the surface of an annulus-shaped ionizer. The ionizer efficiency is nearly 50% since all of the trajectories from the front face of the annulus strike the region from which the negative-ion beam emerges. The calculated sputtering rate on axis is more than four times that for the original SNICS geometry.

References

1. G.T. Caskey, R.A. Douglas, H.T. Richards, and H.V. Smith, Jr., *Bull. Am. Phys. Soc.* **23** (1978) 541; and J.H. Billen and H.T. Richards, *Proceedings of the Symposium of Northeastern Accelerator Personnel CONF-781051* (Oak Ridge, Tenn. 1978) 137.
2. G.T. Caskey, R.A. Douglas, H.T. Richards, and H.V. Smith, Jr., *Nucl. Instrum. & Meth.* **157** (1978) 1.
3. R. Middleton, *Proceedings of the Symposium of Northeastern Accelerator Personnel CONF-781051* (Oak Ridge, Tenn. 1978) 114; and R. Middleton, *Proceedings of the Symposium of Northeastern Accelerator Personnel* (Madison, Wis. 1980) 134.
4. B.A. Carré, *Comp. Journ.* **4** (1961) 73.
5. P. Sigmund, *Phys. Rev.* **184** (1969) 383.